Demonstration of a functional quantum-dot cellular automata cell

Islamshah Amlani,[a] Alexei O. Orlov, Gregory L. Snider, Craig S. Lent, and Gary H. Bernstein
Department of Electrical Engineering, University of Notre Dame, Notre Dame, Indiana 46556

(Received 29 May 1998; accepted 16 September 1998)

We report an experimental demonstration of a functional cell for quantum-dot cellular automata (QCA), a transistorless approach to implement logic functions. The four-dot QCA cell is defined by a pair of series-connected, capacitively coupled input and output double dots. We demonstrate that, at low temperature, an electron switch in the input double dot induces an opposite electron switch in the output double dot, resulting in a complete polarization change of the QCA cell. Switching is verified by electrometer signals which are coupled to the output double dot. Experimental results suggest that electron motion in the coupled double dots is strongly correlated and can support high operating frequencies. Agreement between theoretical predictions and experimentally measured values of the dot potentials is excellent. © *1998 American Vacuum Society*. [S0734-211X(98)13106-2]

I. INTRODUCTION

The microelectronics industry has made amazing progress in the past three decades. Underlying this dramatic growth is the ability to scale down field effect transistors (FETs) which are operated as current switches to store or remove charge from capacitors. Although conventional technology may continue to thrive for some time, staggering obstacles are inevitable as the device feature sizes and gate lengths encroach upon quantum limits. Quantization of charge in both the channel and the doping layer will severely limit the performance of these devices. In contrast, an alternate architecture, known as quantum-dot cellular automata (QCA),[1–4] exploits the intrinsic quantum nature of nanostructures, and may enable scaling to continue unimpeded down to molecular sizes. In this radically new approach to computation, the information is encoded in the position of electrons arranged in an array of cells formed by coupled dots. QCA architecture is a planar technology that does not rely on multilevel interconnects and holds the promise of lower power delay product as well as higher speeds.

One possible form of a basic cell of QCA architecture is shown schematically in Fig. 1(a). The capacitance of each dot within the cell is sufficiently small to ensure charge quantization.[5] In the embodiment investigated here, tunneling is allowed only in the vertical direction of the cell (shown by the line connecting the dots) and the interaction in the horizontal direction is due to Coulombic fields. If each dot pair is charged with one extra electron, the electrons will occupy opposite diagonal sites due to mutual electrostatic repulsion. QCA operation is invoked by applying input gate biases that flip the polarization of the cell as depicted in Fig. 1(b). The two ground states of the cell can be used to represent binary values in digital logic. All Boolean logic functions can be realized by an appropriate arrangement of these basic cells.

The operation of a QCA cell has been recently demonstrated in a four-dot system formed by a pair of single dots and a double dot.[6] It has also been established that two single electron transistors can be used to measure small variations of an electron charge (e) in a capacitively coupled double dot.[7] Here, we consider a six-dot system consisting of a pair of double dots and two single dots. The design of the QCA cell implemented here is more symmetric than the previous four-dot system since it is based on two capacitively coupled identical double dots. In addition to the demonstration of QCA operation, we also discuss experiments that suggest that QCA switching responds to instantaneous potential fluctuations.

II. EXPERIMENT

A schematic diagram of our six-dot QCA system is depicted in Fig. 2(a). It consists of a pair of double dots, referred to as input (D_1-D_2) and output (D_3-D_4) double dots. Coupling capacitors C_{C1} and C_{C2} serve to enhance the electrostatic coupling between the input and the output double dots. Each dot of the output double dot, D_3 and D_4, is also capacitively coupled to a single dot, labeled E_1 and E_2, respectively, which act as electrometers. Each dot of the QCA system is also capacitively coupled to a gate electrode through a capacitor C_1-C_6.

Sample preparation consisted of optical and electron beam lithography on an oxidized Si wafer. Two levels of optical lithography are used to define metal (Au/Pt) interconnect lines and bonding pads. Fabrication of nanometer-scale $Al/AlO_x/Al$ tunnel junctions was accomplished using the standard Dolan-bridge technique.[8] Al islands and leads are defined by electron beam lithography and subsequent shadow evaporation processes with an intermediate *in situ* oxidation step. Figure 2(b) is a scanning electron micrograph of the finished device. The area of the fabricated $Al/AlO_x/Al$ tunnel junctions is approximately 50×50 nm^2. Room temperature tunnel resistance of the junctions, based on current–voltage (I–V) measurement, is about 750 kΩ.

[a]Electronic mail: Islamshah.amlani.1@nd.edu

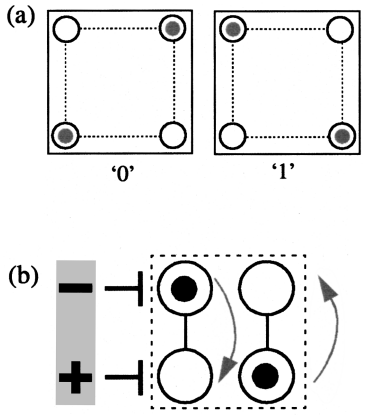

FIG. 1. (a) QCA cell showing the two possible polarizations. (b) Polarization change in the QCA cell under the influence of input gate bias.

The sample is mounted on the cold finger of a dilution refrigerator with a base temperature of 10 mK. Conductances of the double dots and electrometers are measured using standard ac lock-in techniques with an excitation voltage of 3 μV at 25–40 Hz. The experiment is performed in a magnetic field of 1 T to suppress the superconductivity of Al metal at millikelvin temperatures. The capacitance of the tunnel junctions, extracted from the charging energy of the electrometers, is approximately 240 aF. The other lithographic and parasitic capacitances are obtained from the Coulomb blockade oscillations of the double dots and electrometers. Measured capacitance parameters are used in our theoretical simulations of the device characteristics.

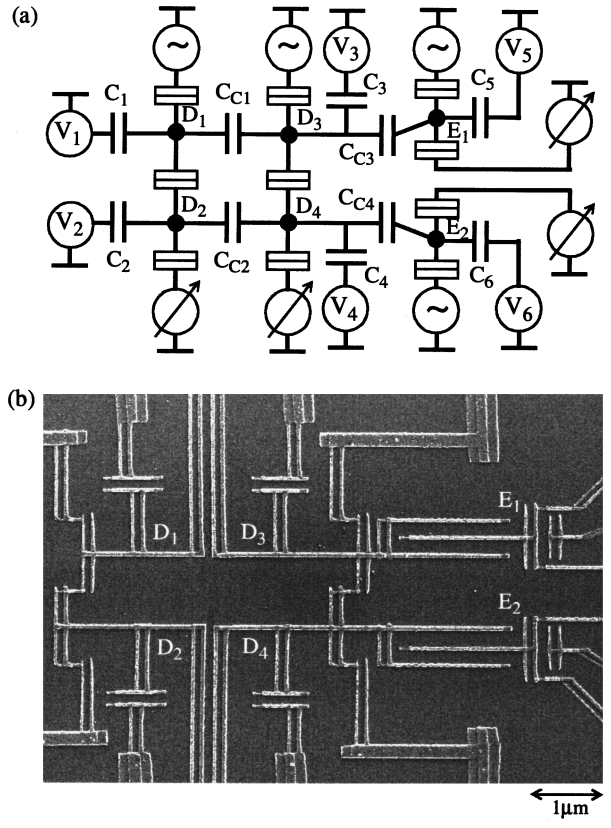

FIG. 2. (a) Schematic diagram of the device structure. (b) Scanning electron micrograph of the device.

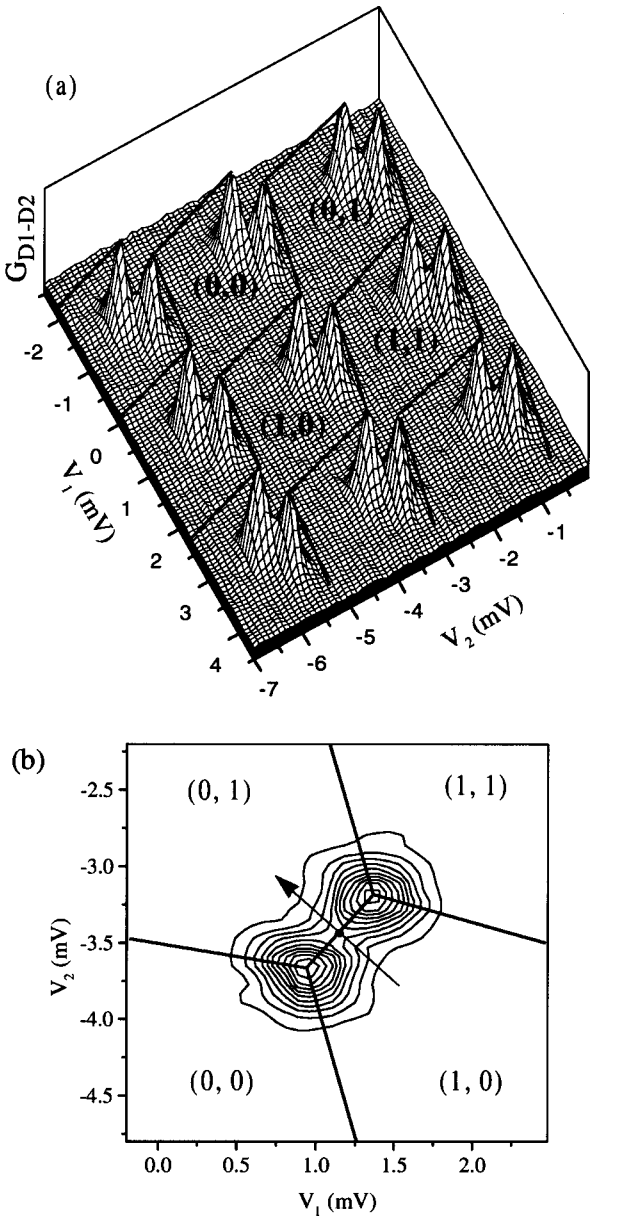

FIG. 3. (a) Charging diagram of the input double dot as a function of the gate voltages V_1 and V_2. Charge configurations (n_1 and n_2), respectively, which represent the number of extra electrons on D_1 and D_2, are arbitrarily chosen. (b) Smaller sections of the charging diagram in the form of a contour plot.

III. RESULTS AND DISCUSSIONS

A. QCA operation

In order to understand the QCA operation, we need to first consider the charging diagram of a double dot. Figure 3(a) shows a surface plot of the conductance of the input double dot in V_1-V_2 space. Each conductance peak in the charging diagram splits due to the interdot electrostatic coupling between D_1 and D_2. Different charge states of the system can be delineated by connecting these split peaks, as demon-

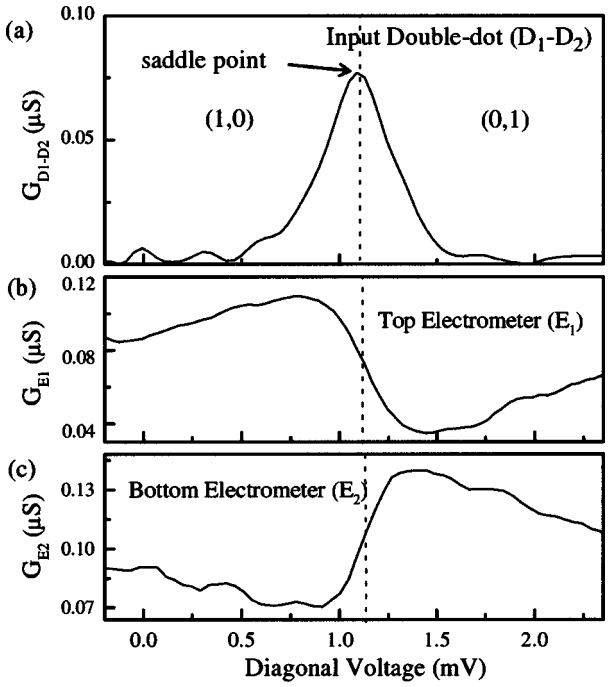

FIG. 4. (a) Conductance of the input double dot as a function of the diagonal voltage along the switching direction indicated by the arrow in Fig. 3(b), and electrometer signals for the (b) top and (c) bottom electrometers.

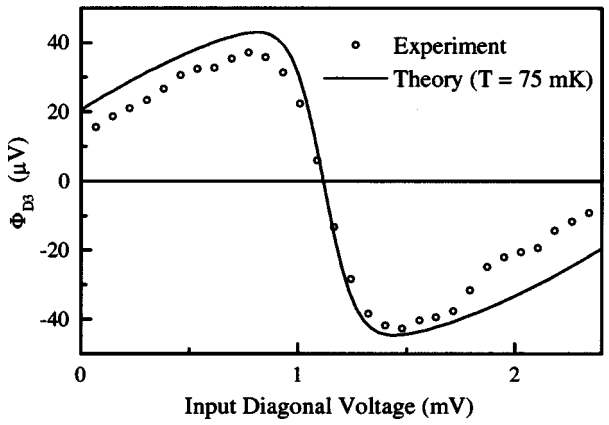

FIG. 5. Experimental and theoretical curves showing potential changes in dot D_3 at 75 mK.

strated by the solid lines. Thus, the charging diagram as a function of the applied biases can be used to map out different electron configurations of the double dot. The excess dot populations (n_1,n_2) in the regions where they are stable are referred to as the ground state for those particular settings of voltages with n_1 and n_2 representing the number of extra electrons on dots D_1 and D_2, respectively. Instability in the electron configurations occurs at the peaks where three different charge states are degenerate leading to a current flow through the system. Away from the peaks, there is no current flow through the double dot due to the Coulomb blockade of electrons. A nonzero conductance between the split peaks, forming a saddle point, is due to a contribution from the nearby states, which are accessible due to a finite thermal energy. Figure 3(b) shows a smaller section of the input double-dot charging diagram in the form of a contour plot. Under the influence of gates V_1 and V_2, the charge configuration of the double dot can be changed by crossing a border between two different charge states. In particular, crossing the border along the ''switching'' direction [shown by the arrow in Fig. 3(b)] results in an electron switch from D_1 to D_2, hence changing the polarization state of the input double dot.

At the polarization change of the input double dot, each dot undergoes a sharp potential change.[9] This is induced by an electron entering or exiting the dot, with the magnitude of the potential shift determined by the capacitances of the dots. These abrupt potential shifts act as additional gate voltages as seen by the output double dot, coupled via capacitors C_{C1} and C_{C2}. If the output double dot, which has a similar charging diagram in V_3-V_4 space as the one in Fig. 3, is biased near the charge exchange border (bias point), the sharp potential shifts induced by the input double dot may be sufficient to pull the *bias* point to the other side of the border. This is possible because, being biased at the saddle point, the output double dot is in its most unstable state. The sharp shift in the bias point from one side of the charge exchange border to the other results in an opposite polarization switch of the output double dot, which is reflected in the conductances of the electrometers.

Figure 4(a) shows the conductance of the input double dot along the charge exchange direction as indicated by the arrow in Fig. 3(b). The peak in the conductance is the saddle point between the (split) peaks and serves as a marker of the border between the (1,0) and (0,1) states. The effect of potential shifts of the input double dot on the output double-dot charge state is reflected in the electrometer conductances, which are sensitive to small local charge excursions on their capacitively coupled dots, mimicking the potential variations of the output double dot D_3-D_4. Figures 4(b) and 4(c) show the conductances of the top and bottom electrometers, respectively. An opposite sharp reset in each electrometer conductance, coincident with an electron switch in the input double dot [Fig. 4(a)], are indicative of a polarization switch of the output double dot.[7] An abrupt downward shift in the conductance of E_1 represents the addition of an electron on D_3. Likewise, an abrupt upward shift in the conductance of E_2 denotes the removal of an electron from D_4. Hence, the data in Fig. 3 show a controlled polarization change of the QCA cell.

Figure 5 shows theoretical and experimental curves of the potential change on D_3 as a function of the input diagonal voltage. The experimental plot for the potential on D_3, Φ_{D_3}, is computed using the electrometer conductance and the capacitance parameters. In the simulation, we use all interdot, dot-to-gate, and dot-to-ground capacitances as measured prior to the experiment. The theoretical results are obtained by minimizing the classical electrostatic energy of the whole system of dots and the voltage leads. Minimum energy charge configurations are calculated subject to the condition that the charge on each dot of the QCA cell be an integer

multiple of *e*. Finite temperature effects are incorporated by thermodynamic averaging over all nearby charge configurations. As can be seen, the agreement between experimental and theoretical results is excellent, with only the substrate background charge and temperature as fitting parameters. Background charge adds only an offset in the position of the peak and has no influence on the magnitude or the period of the dot potential. The best fit to experiment is obtained for 75 mK, which is in close agreement with the actual device temperature, as verified from the peak shape analysis for different temperatures.[10] The discrepancy in the base temperature of the refrigerator and the actual device temperature, which is commonly observed in low temperature measurements below 100 mK, is most likely due to heating of the electron subsystems and insufficient filtering of the leads.

B. Switching frequency

One important consideration in the implementation of QCA architecture is the maximum switching frequency of the cell. We have conducted a simple experiment to extract some information on the switching frequency. We measure the conductances of the input double dot as a function of the diagonal voltage [as shown in Fig. 4(a)] for various settings of voltages applied to the gates of the output double dot. We notice that when the output double dot is biased at the saddle point (charge exchange border), the conductance peak of the input double dot reduces to approximately 50% compared to the case when the output double dot is biased in Coulomb blockade. As mentioned in the previous section, biasing the output double dot on the saddle point implies that the electron configurations (0,1) and (1,0) are equally favorable and the extra electron has an equal probability to be on either D_3 or D_4. Finite temperature causes electron hopping between D_3 and D_4, resulting in potential fluctuations with a frequency determined by the thermal energy (kT) and the resistance of the tunnel junctions.[11] The input double dot sees these instantaneous potential fluctuations of the output double dot in addition to the dc diagonal voltage on its gates. Since the input double dot responds to these sharp potential swings, its conductance, which was initially only a function of the input diagonal voltage, is now an average of two different conductance values based on the amplitude of the instantaneous potential swings. The effect of this averaging is a reduced conductance peak.

In order to test our model, we superimpose a square wave signal with a 50% duty cycle at 100–10 000 Hz on the dc diagonal bias between the gates of the input double dot. This is intended to mimic the abrupt potential swings caused by the charge fluctuations of the output double dot in the previous experiment. The output double dot is biased in blockade in order to prevent any interference caused by single electron tunneling. Figure 6 shows the normalized conductance peak at the saddle point for the input double dot as a function of the applied charge modulation. The cross in Fig. 6 marks the conductance peak lowering observed in the previous experiment. The observed conductance lowering was frequency independent up to 10 kHz (the cutoff frequency of our experimental setup). The magnitude of the charge modulation caused by the square wave signal that corresponds to the position of the cross in Fig. 6 is in close agreement with the theoretically calculated instantaneous charge variations produced by single electron switching in the output double dot observed in the previous experiment. This provides strong evidence that each double dot responds to the instantaneous potential on the other double dot, and that the switching frequency is that determined by the available thermal energy in the system, which for our device is approximately 13 MHz at the temperature of the experiment.[11] This represents a *lower bound* on the maximum operating frequency of the cell. The *upper bound* is set by the RC time constant of the tunnel junctions, which is greater than 1 GHz for the device measured.

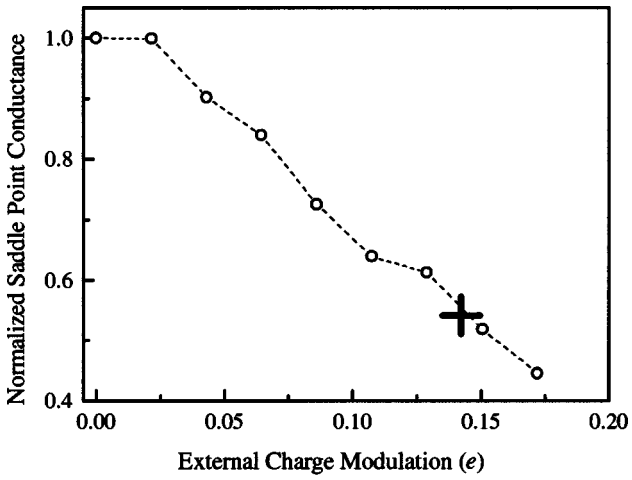

FIG. 6. Normalized conductance peak height at the saddle point for the input double dot as a function of the applied charge modulation amplitude. The *x* coordinate of the cross corresponds to the theoretically calculated charge variation produced by a single electron tunneling from dot D_3 to D_4.

IV. CONCLUSIONS

We have exploited Coulomb blockade effects to demonstrate that the polarization of a QCA cell charged with two extra electrons can be controlled by input gate bias. Switching in the cell is verified experimentally from the electrometer signals, and theoretically by comparing the measured and calculated potential swings in the output double dot. We demonstrated that each double dot is sensitive to instantaneous potential fluctuations induced by single electron switching in the other, capacitively coupled double dot. This implies that coupled double dots can respond to rapid changes of input voltages, suggesting a very high operating frequency of the QCA cell.

ACKNOWLEDGMENTS

This research was supported in part by DARPA, ONR (Grant No. N0014-95-1-1166) and NSF (G. H. B.). The authors wish to thank W. Porod and J. Merz for helpful discussions.

[1]C. S. Lent, P. D. Tougaw, and W. Porod, Appl. Phys. Lett. **62**, 714 (1993).
[2]P. D. Tougaw, C. S. Lent, and W. Porod, J. Appl. Phys. **74**, 3558 (1993).
[3]C. S. Lent, P. D. Tougaw, W. Porod, and G. H. Bernstein, Nanotechnology **4**, 49 (1993).
[4]C. S. Lent and P. D. Tougaw, J. Appl. Phys. **75**, 4077 (1994).
[5]*Single Charge Tunneling*, edited by H. Grabert and M. H. Devoret (Plenum, New York, 1992).
[6]A. O. Orlov, I. Amlani, G. H. Bernstein, C. S. Lent, and G. L. Snider, Science **277**, 928 (1997).
[7]I. Amlani, A. O. Orlov, C. S. Lent, G. L. Snider, and G. H. Bernstein, Appl. Phys. Lett. **71**, 1730 (1997).
[8]T. A. Fulton and G. J. Dolan, Phys. Rev. Lett. **59**, 109 (1987).
[9]P. Lafarge, H. Pothier, E. R. Williams, D. Esteve, C. Urbina, and M. H. Devoret, Z. Phys. B **85**, 327 (1991).
[10]U. Meirav, P. L. McEuen, M. A. Kastner, E. B. Foxman, A. Kumar, and S. J. Wind, Z. Phys. B **85**, 357 (1991).
[11]G. Toth and C. S. Lent (unpublished).